



**HAL**  
open science

## Two-photon absorption-based delivery of nitric oxide from ruthenium nitrosyl complexes

Pascal Lacroix, Isabelle Malfant, Pablo Labra-Vázquez, Norberto Fárfan,  
Gabriel Ramos-Ortiz

► **To cite this version:**

Pascal Lacroix, Isabelle Malfant, Pablo Labra-Vázquez, Norberto Fárfan, Gabriel Ramos-Ortiz. Two-photon absorption-based delivery of nitric oxide from ruthenium nitrosyl complexes. *Dalton Transactions*, 2022, 51 (39), pp.14833-14841. 10.1039/D2DT02553A . hal-03796675

**HAL Id: hal-03796675**

**<https://hal.science/hal-03796675v1>**

Submitted on 4 Oct 2022

**HAL** is a multi-disciplinary open access archive for the deposit and dissemination of scientific research documents, whether they are published or not. The documents may come from teaching and research institutions in France or abroad, or from public or private research centers.

L'archive ouverte pluridisciplinaire **HAL**, est destinée au dépôt et à la diffusion de documents scientifiques de niveau recherche, publiés ou non, émanant des établissements d'enseignement et de recherche français ou étrangers, des laboratoires publics ou privés.

# Two-photon absorption-based delivery of nitric oxide from ruthenium nitrosyl complexes

Pascal G. Lacroix,<sup>a\*</sup> Isabelle Malfant,<sup>a\*</sup> Pablo Labra-Vázquez,<sup>a,b</sup> Norberto Farfan,<sup>b</sup> Gabriel Ramos-Ortiz<sup>c</sup>

<sup>a</sup> *Laboratoire de Chimie de Coordination du CNRS, 205 route de Narbonne, F-31077 Toulouse, France. E-mail : pascal.lacroix@lcc-toulouse.fr, Isabelle.malfant@lcc-toulouse.fr*

<sup>b</sup> *Facultad de Química, Departamento de Química Orgánica, Universidad Nacional Autónoma de México, 04510 México D.F., México.*

<sup>c</sup> *Centro de Investigaciones en Óptica (CIO) A.P. 1-948, 37000 León, Gto. (México)*

**Abstract.** Since the discovery of the numerous physiological roles exhibited by nitric oxide (NO), ruthenium nitrosyl (RuNO) complexes have been regarded as one of most promising NO donors, stable, well tolerated by the body and capable to release NO locally and quantitatively, under light irradiation. This release can be achieved by two-photon absorption (TPA) processes, which allow the irradiation to be performed in the near infrared domain, where light has its maximum depth of penetration in biological tissues. This review provides a short introduction on the biological properties of NO, on RuNO complexes with photo-releasing capabilities, and on the origin of TPA properties in molecules. Then, the RuNO complexes with TPA capabilities are thoroughly discussed either as monometallic or polymetallic species.

## 1. Introduction

The last two decades have witnessed a growing interest for ruthenium nitrosyl complexes. Indeed, a literature survey conducted with the *SciFinder* ACS software program<sup>1</sup> reveals a gradual increase of the number of publications reported annually associated to the keyword “ruthenium nitrosyl”, as shown in Figure 1.

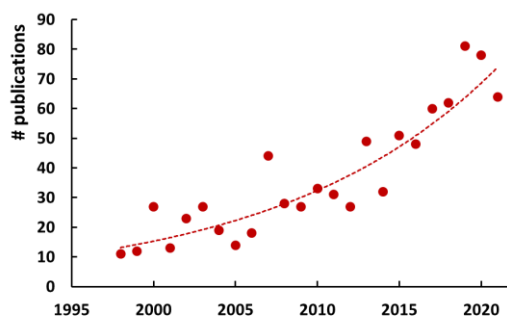


**Fig. 1** Rate of publications reported annually on “ruthenium nitrosyl”

Interestingly, most of these contributions are devoted to the concept of NO release, pointing out the importance of the capabilities exhibited by RuNO complexes to liberate the radical NO<sup>•</sup>. This property appears especially valuable in the context of the gradual discovery of the numerous biological roles devoted to NO<sup>•</sup>,<sup>2-5</sup> thus stimulating the search for strategies aiming at delivering exogenous NO<sup>•</sup> for various biomedical applications. In this context, RuNO complexes have been recognized as the most promising family of NO<sup>•</sup> donors, capable of photo-releasing NO<sup>•</sup> locally and quantitatively on targeted cells, taking advantage of the non-invasive and highly controllable character of light. Furthermore, this capability could find an enhanced interest by use of the two-photon absorption (TPA) technique, which has gained widespread popularity in the biology community and has become an extremely powerful tool for local photoactivation and drug delivery.<sup>6,7</sup>

The present mini-review focuses on the TPA properties of RuNO complexes capable to release NO<sup>•</sup> under optical irradiation. Before addressing this specific topic, a comprehensive introduction of the action and main characteristics of NO<sup>•</sup> in biological environment, the class of RuNO complexes as promising NO<sup>•</sup> donors, and the origin of TPA properties in molecules is provided.

## **2. Nitric oxide: a versatile radical in biological environment**

Until the mid 80's, NO<sup>•</sup> was mainly known as a toxic by-product of gasoline engines and chemical industry. This colorless gas leads to major clinical toxicity at doses  $\geq 80$  ppm,<sup>8</sup> which precludes any beneficial role in biological processes. Nevertheless, things changed completely when it became clear that the endothelium-derived relaxing factor (EDRF), supposed to be a mysterious protein responsible for relaxation of smooth muscle tissues, was surprisingly the simple diatomic molecule of nitric oxide.<sup>9</sup> This discovery led to the title of “molecule of the year” to NO<sup>•</sup> in 1992 by the journal *Science*,<sup>10</sup> followed

by the Nobel prize in medicine awarded to L. J. Ignarro, R. Furchgott, and F. Murad in 1998, “for their discoveries concerning nitric oxide as a signaling molecule in the cardiovascular system”.<sup>11,12</sup> This prestigious recognition drove an intense research interest towards nitric oxide. Indeed, there have been more than 70 000 scientific publications reported on NO<sup>•</sup>, in the last 12 years.<sup>13</sup>

The role of NO<sup>•</sup> in biology has been thoroughly investigated. First applications of nitric oxide in medicine were indirectly reported since the XIXth century. For instance, it was observed by W. Murrell in 1879 that nitroglycerine (*I*, Figure 2), the main component of dynamite, could be an efficient remedy for angina pectoris.<sup>14</sup> In this molecule, commercialized as “Trinitrin”, the role devoted to NO<sup>•</sup> was not evidenced in these early therapeutic applications, but it is now recognized that *I* gradually decomposes in the body, leading to the formation of NO<sup>•</sup>, as the active therapeutic agent.

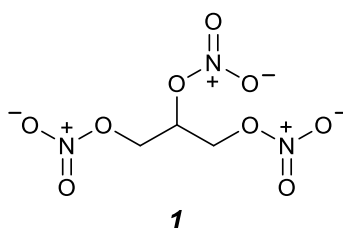


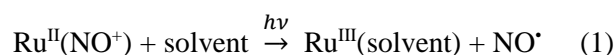
**Fig. 2** The molecule of nitro-glycerin (1,2,3-trinitroxypropane), a well-known NO<sup>•</sup> donor commercialized as “Trinitrine”

The early discoveries of production and physiological application of NO<sup>•</sup> have been reviewed.<sup>15,16</sup> NO<sup>•</sup> is naturally synthesized from L-arginine via the enzyme nitric oxide synthase (NOS).<sup>17</sup> It plays numerous physiological roles such as neurotransmission,<sup>18-20</sup> immunology,<sup>21,22</sup> blood pressure regulation,<sup>23</sup> vasodilatation,<sup>24-26</sup> angiogenesis,<sup>27</sup> among others. Therefore, the use of NO<sup>•</sup> for therapeutic applications has become an area of great interest.<sup>28</sup>

It is worth pointing out that the physiological action of nitric oxide usually depends on its concentration, with antagonist effects in some cases.<sup>29,30</sup> For instance, at concentrations around 10<sup>-6</sup> mol L<sup>-1</sup>, it induces programmed cell death by apoptosis, which can be used as a mechanism for cancer therapy, while it favors cells proliferation at concentrations around 10<sup>-9</sup> mol L<sup>-1</sup> with applications in tissues healing and repair. Due to this versatility, and taking into account its inherent toxicity, the delivery of NO<sup>•</sup> must be perfectly controlled spatially, temporally, and quantitatively to avoid undesirable effects on untargeted cells. These are the reasons why an intense research activity has been devoted to Ruthenium nitrosyl complexes, in the last two decades, as will be developed in the next section.

### 3. Ruthenium nitrosyl complexes as a promising class of NO<sup>•</sup> donors

Nitrosyl complexes have long been investigated in inorganic chemistry with a large panel of applications in catalysis and biochemistry.<sup>31</sup> In material science, they have been investigated for their photoreactivity. They led to bistable species with yields of photoswitch close to 100 % between the nitrosyl (NO) and *iso*-nitrosyl (ON) form, in a RuNO complex of formula [Ru(py)<sub>4</sub>Cl(NO)]<sup>2+</sup>.<sup>32,33</sup> Furthermore, nitrosyl complexes have also become a popular class of NO<sup>•</sup> donors, due to their capability to release NO<sup>•</sup> under optical irradiation, taking advantage of the noninvasive character of light.<sup>34-36</sup> Among them, RuNO complexes offer higher design flexibility and solution stability than oxygen-sensitive FeNO and MnNO species.<sup>37-43</sup> They are usually stable in the dark, thus avoiding the deleterious effect of high concentration of NO<sup>•</sup> radicals spread everywhere in the body, by uncontrolled release. These species undergo the following photoreaction:



The issue of the charge localization is important in this equation. RuNO species are usually described using the Enemark-Feltham notation {Ru(NO)}<sup>n</sup>, which indicates that the sum of  $d_{\text{Ru}}$  and  $\pi^*_{\text{NO}}$  electrons is equal to  $n$ .<sup>44</sup> In the present case  $n = 6$ . Therefore, any situation between Ru<sup>II</sup>(NO<sup>+</sup>) and Ru<sup>III</sup>(NO<sup>•</sup>) can be envisioned. Additionally, there are several possible conformations for ruthenium nitrosyl species: the linear Ru-NO (GS) and Ru-ON (MS1) and the bent Ru-NO (MS2) conformations.<sup>43</sup> In the complexes presented here, the electronic configuration is Ru<sup>II</sup>(NO<sup>+</sup>), which corresponds to linear Ru – N – O species and diamagnetic properties (close shell  $d^6$  configuration). By contrast, NO is invariably released as the neutral radical NO<sup>•</sup>, instead of the nitrosonium cation (NO<sup>+</sup>). This is readily verified by EPR spectroscopy, the best technique to identify NO<sup>•</sup>.<sup>45</sup> It implies that the photo-release process can be regarded grossly as arising from an intense intramolecular charge transfer towards the withdrawing nitrosyl ligand.

It must be mentioned that most of the RuNO complexes absorb in the  $\lambda = 300 - 500$  nm wavelength range, therefore out of the therapeutic window,<sup>46</sup> which corresponds to the range where light has its maximum depth of penetration in biological tissues (between  $\lambda = 600$  nm and  $\lambda = 1300$  nm). To overpass this difficulty, two strategies can be employed to make the electronic transitions of the complexes compatible with the optical therapeutic window: (i) the search of suitable ligands capable of decreasing significantly the energy band gap between ground and excited states, which in turn would induce a red-shift to  $\lambda > 600$  nm in the corresponding absorption spectra, and an enhancement of light absorption in the electronic transitions of the complexes and (ii) the use of the two-photon absorption (TPA) technique.

(i) The dominant contribution in this approach is that of the group of P. K. Mascharak.<sup>37-39,47-49</sup> A representative example illustrating this approach is shown in Figure 3 in which the red-shifting is produced by the use of two ligands of extended  $\pi$ -delocalization: a quinolone-based tetra-dentate N4 ligand and a resorufin dye. In this system, the absorption maximum ( $\lambda_{\max}$ ) reaches 500 nm.<sup>47</sup>

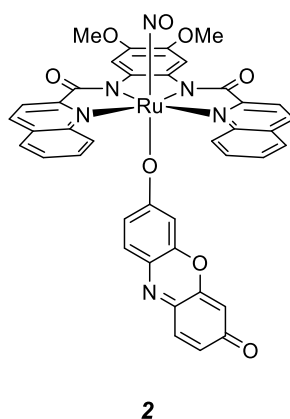


**Fig. 3** RuNO complex with highly conjugated ligands and  $\lambda_{\max}$  value of 500 nm.

(ii) The alternative approach is based on the TPA technique, which has become a widespread tool in numerous biomedical applications.<sup>6,7</sup> In the context of NO<sup>•</sup> delivery, the TPA technique offers unique advantages summarized as follows:

- TPA, in which one photon required at  $\lambda_{\max}$  can be replaced by two photons at  $2 \times \lambda_{\max}$ , allows the irradiation to be performed in the therapeutic window of biological tissues.
- Due to its dependence to the square of the light intensity, the TPA process takes place in the close vicinity of the beam waist of a focused laser, thus avoiding any undesirable effect on untargeted cells.
- This technique avoids the use of UV radiation, which usually leads to irreversible damages in the tissues. Additionally, the TPA is usually achieved by means of a pulsed laser working in the sub-pico ( $< 10^{-12}$  sec.) regime (*vide infra*). Therefore, the energy transferred is negligible, which ensures the absence of any side-effect.

The challenge in this promising approach is to design molecules capable of exhibiting a significant TPA response. Indeed, if the TPA process appears universal, its intensity varies tremendously from molecule to molecule. In this context, most RuNO complexes would provide candidates with negligible efficiencies. The basic requirements for molecules with sizeable TPA capabilities are summarized in the next section.

#### 4. Origin of the TPA properties in molecules

Contrary to the one-photon absorption (OPA) phenomenon, the two-photon absorption (TPA) is a nonlinear optical (NLO) process in which two photons are absorbed simultaneously within a single quantum act. It is therefore different than the excited state absorption (ESA) in which the first absorption of one photon is followed by a second one from the first excited state to a second excited state of higher energy, as shown in Figure 4.

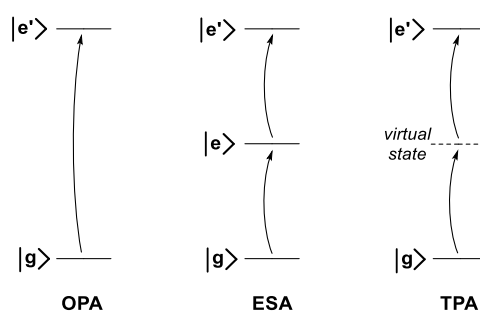


**Fig. 4** Difference between one-photon absorption (OPA) from the ground state ( $g$ ) to an excited state ( $e'$ ), excited state absorption (ESA) in two steps to an excited state  $e'$  occurring during the life time of the first excited state ( $e$ ), and two-photon absorption (TPA) to an excited state ( $e'$ ) where two photons of energy  $\frac{E_{e'} - E_g}{2}$  are absorbed simultaneously.

Various reviews have provided a comprehensive description of the origin of TPA properties in molecules, aiming at a best selection of promising TPA candidates.<sup>6,7,50-52</sup> The intensity of the TPA response is quantified by the molecular cross-section ( $\sigma_{TPA}$ ) expressed in Göppert-Mayer (GM), a coefficient somewhat similar to the OPA extinction coefficient ( $\epsilon$ ).

Ultimately,  $\sigma_{TPA}$  is related to the electronic transition of the molecules.<sup>53</sup> There are commonly two kinds of TPA molecules:

(i) The dipolar (donor/acceptor) systems, in which a simple electronic transition between two states ( $g$ ,  $e$ ) is assumed to provide most of the TPA response, lead to:<sup>50</sup>

$$\sigma_{TPA} \approx \frac{16\pi^2 \mu_{ge}^2 (\mu_{ee} - \mu_{gg})^2}{5\hbar^2 c^2 \Gamma} \quad (2)$$

were  $\mu_{ge}$  is the transition dipole moment of the  $g \rightarrow e$  transition,  $\mu_{gg}$  and  $\mu_{ee}$  the dipole moment in the ground and excited states, respectively, and  $\Gamma$  the linewidth broadening parameter which is often taken at the constant value of 0.1 eV. What is important to emphasize in Equation (2) is the importance of the  $\mu_{ee} - \mu_{gg}$  term, which implies that the molecule must possess the strong charge transfer character usually associated to most standard NLO chromophores. In the case of RuNO species, it will be helped by the fact that the nitrosyl itself is an extremely efficient electron-withdrawing group, which therefore requires the ancillary ligand to behave as a donor in order to enhance the “push-pull” effect towards NO $\cdot$ .

(ii) The quadrupolar centrosymmetric systems, frequently designed as the combination of two *push-pull* dipolar sub-units. In this case, three states ( $g$ ,  $e$ ,  $e'$ ) must necessarily be involved in the simpler case, which leads to:<sup>50</sup>

$$\sigma_{TPA} \approx \frac{4\pi^2 \omega_{ge'}^2}{5\hbar^2 c^2} \frac{\mu_{ge}^2 \mu_{ee'}^2}{(\omega_{ge} - \omega_{ge'}/2)^2 \Gamma'} \quad (3)$$

in which the TPA process takes place towards the second excited state ( $e'$ ). Interestingly, the presence of a  $g \rightarrow e$  transition having energy  $\hbar\omega_{ge}$  close to that of the incident laser beam  $\frac{\hbar\omega_{ge'}}{2}$  leads to the possibility of significant cross-section enhancement due to a nearly vanishing denominator in Equation (3). For this reason, quadrupolar TPA chromophores are potentially more appealing than their parent dipolar species. Importantly, Equations (2) and (3) are valid at resonance, which means that the energy of individual photons of the laser must be half of that of the targeted transition. This indicates that the experimental  $\sigma_{TPA}$  always depends on the photon energy. In the next section, the  $\sigma_{TPA}$  values will always be given at 800 nm, for fair comparative purposes, unless, explicitly specified.

## 5. Ruthenium nitrosyl complexes with TPA capabilities

There are basically two approaches in the design of RuNO complexes capable of releasing NO $\cdot$  under TPA irradiation: (i) the use of a TPA antenna, which can induce the release by energy transfer to the RuNO unit, and (ii) the design of a new RuNO complex in which NO acts as an efficient withdrawing group. Both strategies are illustrated in Figure 5.



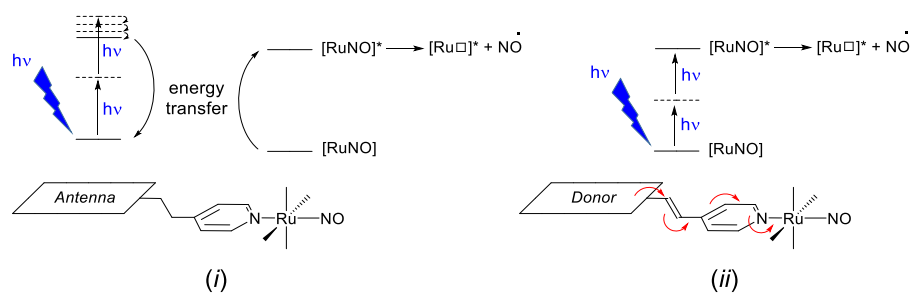


**Fig. 5** The two strategies envisioned to initiate the NO\* release by a two-photon process: (i) by using a TPA antenna, and (ii) from a TPA complex in which RuNO acts as the withdrawing group.

The first picture (i) requires an antenna, which refers to a fragment of the ligand bearing both ground and excited state electron densities, without any electronic contribution of the rest of the complex. Additional requirements for the antenna are the fact to possess a large cross-section ( $\sigma_{\text{TPA}}$ ) and to be fluorescent at the wavelengths of absorption of the RuNO unit. After the TPA absorption, an energy transfer occurs to the RuNO complex, which is assumed to release NO\* in the excited state [RuNO]\*. Few investigations have been reported on iron-nitrosyl complexes, in which TPA antenna were grafted.<sup>36,54-56</sup> Nevertheless, and to the best of our knowledge, it was never employed for RuNO species. A limiting factor in this approach may be related to the fact that the antenna should necessarily absorb in a range of wavelength shorter than that of the RuNO complex (Figure 5). That would imply to design a TPA antenna with  $\lambda_{\text{max}}$  around 300 nm. Being related to long-range  $\pi$ -delocalized structures, TPA chromophores with large  $\sigma_{\text{TPA}}$  values would more likely absorb at larger wavelength. By contrast, our group has developed the alternative approach (ii) (Figure 5), where the RuNO complex itself behaves as the TPA material and as the NO\* donor. We will report first on the attempts conducted within the class of dipolar molecules (Equation 2), and finally on the promising results obtained on polymetallic species (Equation 3).

### 5.1. Dipolar RuNO complexes

As mentioned above (Section 4), the ancillary ligand must necessarily be an electron donor to ensure the strong charge transfer toward NO required in dipolar TPA systems (Equation 2). In our first attempt, we selected a fluorenyl-substituted terpyridine ligand (FT, Figure 6), in which the fluorenyl is an electron-rich fragment frequently employed in the search of efficient TPA chromophores.<sup>57-61</sup> The resulting [FTRuCl<sub>2</sub>(NO)]<sup>+</sup> complex **3** exhibits the strong *push-pull* character, evidenced from the frontier (HOMO-LUMO) orbitals shown in Figure 6.<sup>62</sup> Additionally, careful examination of the unoccupied (LUMO) level reveals interesting electronic features:

- the ruthenium nitrosyl overlap has a clear antibonding character, leading to a weakening of the bond strength between the ruthenium and nitrogen atoms during the transition.
- the transition leads to an intense electron transfer to the  $\text{NO}^+$  ligand, which grossly corresponds to the situation depicted in Equation (1).

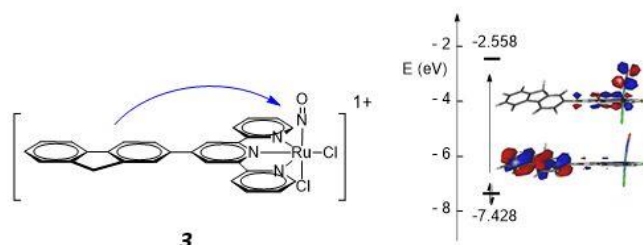
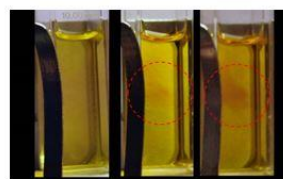


**Fig. 6** Ruthenium nitrosyl complex ( $[\text{FTRuCl}_2(\text{NO})]^+$ ) (**3**) with frontier orbitals (HOMO-LUMO) illustrating the strong *push-pull* intramolecular charge transfer (blue arrow) between the electron-rich fluorene and the acceptor RuNO unit (from ref. 62).

At first, both observations seem to favor the direct  $\text{NO}^*$  release process. Therefore, a strong *push-pull* character would enhance both  $\text{NO}^*$  release and TPA properties, and therefore be highly desirable. Nevertheless, we have observed that a RuNO complex built up from a very poorly donating ligand (*e.g.* nitrophenyl-terpyridine), in which the *push-pull* effect nearly vanishes, provides a rather efficient  $\text{NO}$  release.<sup>63</sup> Further investigations of optical properties of RuNO complexes came to the conclusion that a single  $[\text{RuNO}] \rightarrow [\text{RuNO}]^*$  transition could hardly account for the photochemical properties of RuNO.<sup>64</sup>

Interestingly, theoretical investigations support the idea that the first excited state is not a dissociative state, but is likely stabilized as a meta stable state, thus requiring a second electron transition to efficiently release  $\text{NO}^*$ .<sup>65</sup> Although the investigation of the mechanism falls out of the scope of the present review, it is worth pointing out that large TPA response, by virtue of significant *push-pull* character does not necessarily imply efficient  $\text{NO}^*$  release. Finally, the  $\sigma_{\text{TPA}}$  measured at 800 nm was found to be equal to 100 GM.<sup>66</sup> The fact that the release is indeed initiated by TPA irradiation has been verified experimentally (Figure 7).<sup>67</sup> It requires the use of the Griess test, which involves an *in situ* oxidation of the released  $\text{NO}^*$  to  $\text{NO}_2^-$ , followed by a reaction with sulfanilic acid, and finally the formation of a pink azo dye ( $\lambda_{\text{max}} = 548 \text{ nm}$ ).<sup>68</sup>



(a) (b) (c)

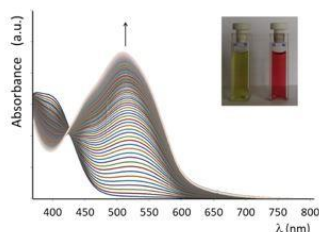


**Fig. 7** Top:  $\text{NO}^+$  release from **3** under TPA at 810 nm detected by the Griess test with irradiation time of 0 min (a), 10 min (b), and 30 min (c). Bottom: Spectroscopic confirmation of  $\text{NO}^+$  within the Griess test with the appearance of a pink dye around 550 nm (ref. 62, 67).

The purpose of such species being to be ultimately used in biological environment, where many undesirable species could replace the labile chloride ligands, an alternative complex built up from a robust bipyridine was envisioned. An additional advantage of using bipyridine comes from the fact that it avoids the frequent mixture of *trans*-(Cl,Cl) and *cis*-(Cl,Cl) isomers present in the synthesis of [(terpyridine)RuCl<sub>2</sub>(NO)]<sup>+</sup> complexes, and the tedious purification process, unsustainable in some cases. The resulting complex (**4**, Figure 8) exhibits the same properties as **3**. In particular, the HOMO level is strictly pinned on the fluorene moieties in both complexes. The cross-section of **4** is equal to 108 GM, which indicates that the bipyridine does not contribute to the TPA properties.<sup>66</sup>

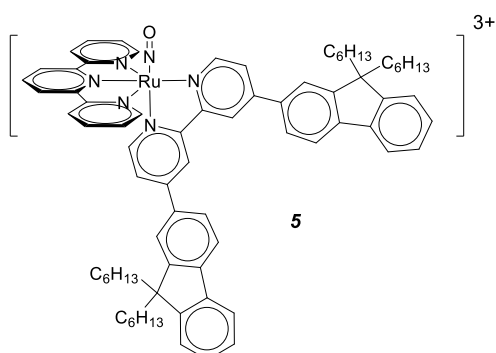
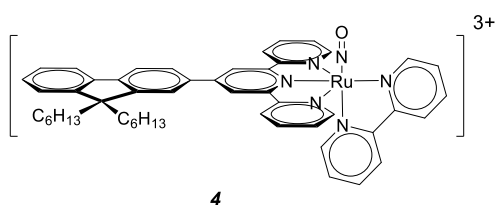


**Fig. 8** Ruthenium nitrosyl complexes with fluorene substituent on various positions on the  $[\text{Ru}(\text{terpy})(\text{bipy})(\text{NO})]^{3+}$  core.

It should be noted that the TPA measurements are usually performed by means of the two-photon excited fluorescence (TPEF), a technique which requires for the chromophores to be fluorescent at least to some extent.<sup>69,70</sup> Unfortunately, the present RuNO species exhibit very weak fluorescence and the Z-scan technique is preferable,<sup>71</sup> which requires high concentration of chromophores (up to  $10^{-2}$  mol L<sup>-1</sup>) to ensure a suitable signal / noise ratio. To reach this goal, hexyl chains are usually added on the fluorenyl substituents. Nevertheless, they are not involved in the  $\pi$ -conjugated skeleton, and do not modify the TPA response.

With 5 pyridine units coordinated to the ruthenium center of **4**, the issue of the best position for grafting the fluorene ligand is naturally addressed. Complex **5**, in which two fluorenes are present on the bipyridine moieties leads to a slight enhancement of  $\sigma_{\text{TPA}}$  to 156 GM.<sup>72</sup> This modest result was obtained by means of a tedious synthetic work, therefore the next research efforts have focused on substitutions performed on the terpyridine fragment only.

In *push-pull* TPA materials, the possibility to enhance the properties requires either (i) an increase of the donating/accepting capabilities of the molecule or (ii) an elongation of the  $\pi$ -conjugated bridge between the donor and the acceptor units. The first strategy (i) was envisioned with the use of carbazole (Figure 9), an organic structure related to the fluorene species in which a nitrogen atom can provide an enhancement of the donating character.

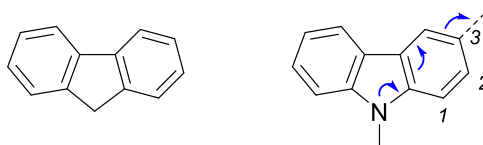


**Fig. 9** Two related electron-rich fragments: fluorene (left) and carbazole (right).

However, to take full advantage of this possibility, the carbazole must be grafted in the *trans* position to the terpyridine (3 in Figure 9), which leads to the bent complex **6** (Figure 10).<sup>73</sup>

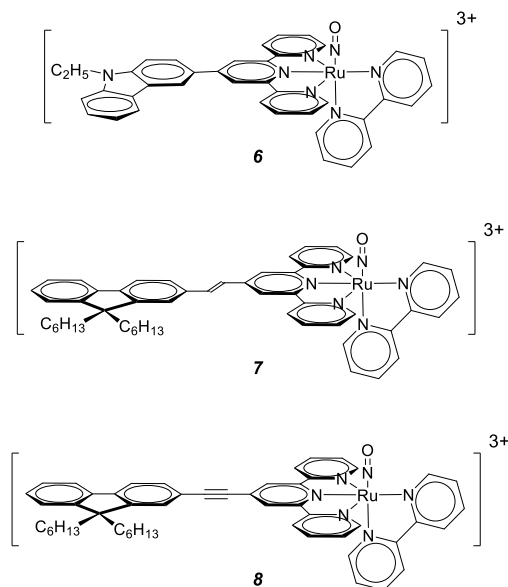


**Fig. 10** RuNO complexes tested in an attempt to enhance the *push-pull* effect induced by the fluorenylterpyridine ligand.

Complex **6** exhibits a significant increase of cross-section, under irradiation at 800 nm, with  $\sigma_{\text{TPA}} = 159$  GM, compared to the  $\sigma_{\text{TPA}} = 108$  GM measured in **4**.<sup>73</sup> At the theoretical level, a TD-DFT computation allows to verify the nature of the orbitals involved in the electronic transitions of the species.<sup>74</sup> In particular, the HOMO level, centered on the donating substituent of **6** is located 0.4 eV above that of **4**, which leads to a red-shift of the transition of **6**. The resulting increase of the transition dipole moment  $\mu_{ge}$  (Equation 2) accounts qualitatively for this enhancement.

The second approach (*ii*) to enhance the TPA properties, is based on the fact that the size of a chromophore has a strong effect on its TPA response.<sup>7</sup> In the case of *push-pull* systems, a representative example is provided in Figure 11, to illustrate the well known tendency for larger  $\sigma_{\text{TPA}} / N_e$  value ( $N_e$  being the number of  $\pi$ -electrons in the bridge) as the size of the molecule increases.<sup>75</sup>

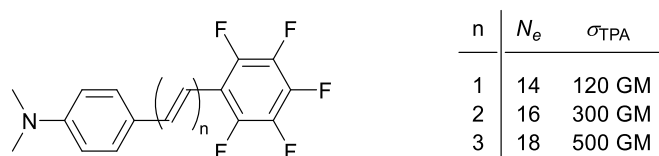


**Fig. 11** Influence of the length of the chromophore (number of  $\pi$ -electrons  $N_e$ ) on the TPA response.

In order to check this effect on the RuNO complexes, compounds **7** and **8** have been compared to **4**. They lead to modest enhancement of cross-sections with  $\sigma_{\text{TPA}}$  values of 131 GM and 150 GM, for **7** and

**8**, respectively.<sup>76</sup> Clearly, the effect of the bridge along the **4**, **7**, **8** series is surprisingly weak, compared to that observed in the fluorinated species gathered in Figure 11. Altogether, the synthetic modifications achieved on the reference complex **4**, lead to  $\sigma_{\text{TPA}}$  values at best twice that of the reference, which encourage to extend the investigation to complexes of greater complexity than those of the dipolar family.

## 5.2. Octupolar RuNO complexes

Octupolar architectures, which are non polar species with 2- or 3-dimensional polarizabilities, allowed the design of chromophores with very large NLO responses.<sup>77</sup> In two-photon absorption, quadrupolar species can frequently be regarded as double donor-acceptor systems (DA...AD or AD...DA). Without interaction between the sub-units, the properties of the quadrupole arise from the sum of those of its independent DA components. This situation is not relevant in material science. By contrast, when some interactions take place within the quadrupole, the resulting TPA response can be strongly enhanced. Before reporting the properties of symmetrical bimetallic RuNO species, it must be recalled that a transition active at one photon (OPA) in a centrosymmetric point group is necessarily TPA silent, and vice versa. For this reason, OPA and TPA spectra may be significantly different in quadratic chromophores. This is illustrated in Figure 12.

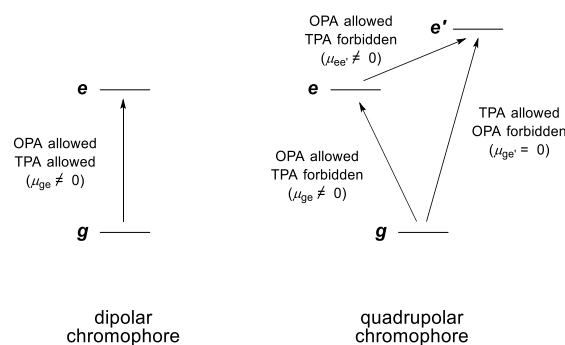


**Fig. 12** OPA and TPA allowed and forbidden transitions in *push-pull* (left) and centrosymmetric (right) molecules. The *g*, *e*, and *e'* states correspond to those of Equations (2) and (3).

A family of bimetallic RuNO species has been investigated in which the fluorenylterpyridine ligand is used as the bridge between the equivalent RuNO sub-units.<sup>78</sup> The resulting complexes **9-11** are shown in Figure 13. Compounds **9** (point group  $C_1$ ) and **10** (point group  $C_2$ ) are non-centrosymmetric, but can be regarded as pseudo-centrosymmetric. Therefore, the quadratic model (Figure 12 and Equation 3) may be applicable to them, at least to some extent. Compound **11** is  $C_i$  (centrosymmetric). These species with

extended  $\pi$ -conjugated structures possess UV-visible spectra exhibiting red-shifted absorption maxima and higher intensities than those of the parent compound **4**, which indicate some degree of interaction through the conjugated bridges. Their TPA cross sections are clearly enhanced with  $\sigma_{\text{TPA}}$  equal to 401 GM, 185 GM and 309 GM, for **9**, **10**, and **11**, respectively. Furthermore, they reveal an additional TPA response at higher energy ( $\lambda = 700$  nm) with  $\sigma_{\text{TPA}}$  equal to 1182 GM, 732 GM, and 1523 GM, for **9**, **10**, and **11**, respectively. Interestingly, the overall red-shift evidenced in these highly delocalized species makes this high energy wavelength compatible with the therapeutic window, which provides a significant breakthrough.

Increasing the dimensionality of RuNO chromophores was definitely established as the best strategy towards efficient TPA materials with the investigation of the 3-arm compound **12** (Figure 13).<sup>79</sup> The theoretical investigation of TPA species in  $C_3$  geometry was previously reported, and was found to derive from the *push-pull* effect present in a single arm.<sup>80</sup> Without interaction between the arms, the resulting cross-section is equal to 3 times that of a single arm (close to  $3 \times 108$  GM in reference to **4**). By contrast, the central truxene ligand in **12** encompasses three fluorene intricate units in an extended  $\pi$ -structure of greater complexity than that of the parent fluorene. Consequently, the TPA response of **12** reaches  $\sigma_{\text{TPA}} = 1\,600$  GM at 800 nm,<sup>79</sup> the highest cross-section reported to date for a ruthenium nitrosyl complex.

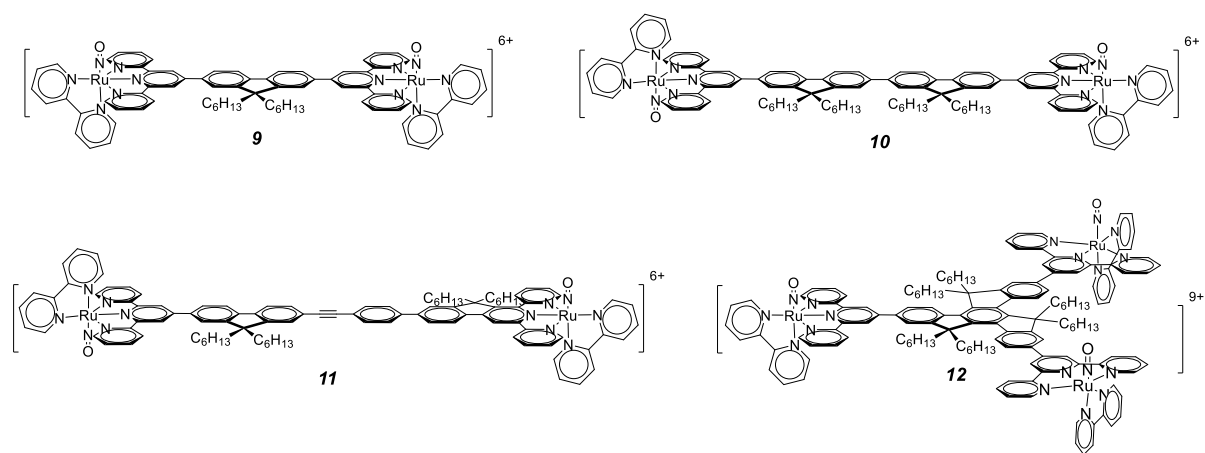


**Fig. 13** Bi- and trimetallic RuNO complexes with extended  $\pi$ -delocalized skeletons.

## 6. Concluding remarks

In the last 5 years, significant progresses have been achieved on the search for RuNO complexes capable of releasing NO $\cdot$  by means of a TPA excitation, with  $\sigma_{\text{TPA}}$  cross-sections enhanced from 100 GM in **3**

to 1 600 GM in *I2*. It is now established that the strategy based on increasing the dimensionality to reach the largest cross sections is the most promising. Values higher than 1 500 GM for such species lie in the range of the best ruthenium complexes,<sup>81</sup> for this size of molecules. In parallel, the research must be developed towards NO<sup>•</sup> carriers of much larger sizes, for instance incorporated into dendrimeric species or into micelles in which hundreds of RuNO units could be embedded. Another research effort is currently in progress to test the efficiency of the RuNO complexes in biological medium either as anti-tumoral<sup>69</sup> or bactericide agents.<sup>82</sup>

### Conflicts of interest

There are no conflicts of interest to declare.

### Acknowledgements

The authors thank the *Centre National de la Recherche Scientifique* (CNRS - France) and the *Consejo Nacional de Ciencia y Tecnología* (CONACYT – México) for financial supports through the International French-Mexican Laboratory LIA-LCMMC and through the International Research Program IRP-MCCM.

### References

- 1 <https://www.cas.org/solutions/cas-scifinder-discovery-platform/cas-scifinder>
- 2 L. J. Ignarro, *Nitric Oxide Biology and Pathobiology*, Academic Press, San Diego, **2000**.
- 3 B. Bonavida, *Nitric Oxide and Cancer: Prognosis, Prevention and Therapy*, Springer, New-York, **2010**.
- 4 A. W. Carpenter, M. H. Schoenfisch, *Chem. Soc. Rev.*, **2012**, *41*, 3742-3752.
- 5 P. C. Ford, *Nitric Oxide*, **2013**, *34*, 56-64.
- 6 B. Strehmel, V. Strehmel, *Adv. Photochem.*, **2007**, *29*, 111-341.
- 7 M. Pawlicki, H. A. Collins, R. G. Denning, H. L. Anderson, *Angew. Chem. Int. Ed.*, **2009**, *48*, 3244-3266.
- 8 D. Davidson, E. S. Barefield, J. Kattwinkel, G. Dudell, M. Damask, R. Straube, J. Rhines, C. T. Chang, *Pediatrics*, **1998**, *101*, 325-334.
- 9 S. Moncada, R. M. J. Palmer, E. A. Higgs, *Hypertension*, **1988**, *12*, 365-372.
- 10 D. E. Koshland, *Science*, **1992**, *258*, 1861.



- 11 L. J. Ignarro, *Angew. Chem. Int. Ed.*, **1999**, 38, 1882-1892.
- 12 <https://www.nobelprize.org/prizes/medecine/1998/summary/>
- 13 N. Hogg, Editor in chief of *Nitric Oxide* (<https://www.nitricoxidesociety.org/our-impact>)
- 14 W. Murrell, *Lancet*, **1879**, 1, 80-81.
- 15 J. R. Lancaster, *Biochem. Pharmacol.*, **2020**, 176, 113793.
- 16 K. Bian, M.-F. Doursout, F. Murad, *J. Clin. Hypertens.*, **2008**, 10, 304-310.
- 17 G. Walford and J. Loscalzo, *J. Thromb. Haemostasis*, **2003**, 1, 2112-2118.
- 18 D. S. Bredt, P. M. Hwang, S. H. Snyder, *Nature*, **1990**, 347, 768-770 .
- 19 J. Garthwaite, *Trends Neurosci.*, **1991**, 14, 60-67.
- 20 J. Garthwaite, *Trends Neurosci.*, **1995**, 18, 51-52.
- 21 J. B. Hibbs Jr., R. R. Taintor, Z. Vavrin, E. M. Rachlin, *Biochem. Biophys. Res. Commun.*, **1988**, 157, 87-94.
- 22 M. A. Marletta, P. S. Yoon, R. Iyengar, C. D. Leaf, J. S. Wishnok, *Biochemistry*, **1988**, 27, 8706-8711.
- 23 D. Alonso, M. W. Radomski, *Heart Failure Rev.*, **2003**, 8, 47-54.
- 24 R. A. Cohen, R. M. Weisbrod, M. Gericke, M. Yaghoubi, C. Bierl, V. M. Bolotina, *Circ. Res.*, **1999**, 84, 210-221.
- 25 B. W. Allen, J. S. Stamler, C. A. Piantadosi, *Trends Mol. Med.*, **2009**, 10, 452-460.
- 26 Y. Zhao, P. M. Vanhoutte, S. W. S. Leung, *J. Pharm. Sci.*, **2015**, 129, 83-94.
- 27 L. Morbidelli, S. Donnini, M. Ziche, *Curr. Pharm. Des.*, **2003**, 9, 521-530.
- 28 A. W. Carpenter, M. H. Schoenfisch, *Chem. Soc. Rev.*, **2012**, 41, 3742-3752
- 29 D. D. Thomas, L. A. Ridnour, J. S. Isenberg, W. Flores-Santana, Ch. H. Switzer, S Donzellie, P. Hussain, C. Vecoli, N. Paolocci, S. Ambs, C. Colton, C. Harris, D. D. Roberts, D. A. Wink, *Free Radic. Biol. Med.*, **2008**, 45, 18-31.
- 30 S. Mocellin, V. Bronte, D. Nitti, *Med. Res. Rev.* 2007, 27, 317-352.
- 31 *Nitrosyl complexes in Inorganic Chemistry, biochemistry and medicine*. D. Michael, P. Mingos Eds. *Structure and Bonding* (Berlin, Germany) **2014**, 153 and 154.
- 32 B. Cormary, I. Malfant, M. Buron-Le Cointe, L. Toupet, B. Delley, D. Schaniel, N. Mockus, T. Woike, K. Fejfarova, V. Petricek, M. Dusek, M., *Acta Crystallogr. Sect. B* **2009**, 65, 612-623
- 33 D. Schaniel, B. Cormary, I. Malfant, L. Valade, T. Woike, B. Delley, K. W. Kraemer, H.-U. Guedel, *Phys. Chem. Chem. Phys.* **2007**, 9, 3717- 3724
- 34 J. M. Mir, B. A. Malik, R. C. Maurya, *Rev. Inorg. Chem.*, 2019, 2, 91-112.
- 35 A. D. Ostrowski, P. C. Ford, *Dalton Trans.*, **2009**, 10660-10669
- 36 P. C. Ford, *Acc. Chem. Res.*, **2008**, 41, 190-200
- 37 M. J. Rose, P. K. Mascharak, *Curr. Opin. Chem. Biol.*, **2008**, 12, 238-244.
- 38 N. L. Fry and P. K. Mascharak, *Acc. Chem. Res.*, **2011**, 44, 289-298

- 39 M. J. Rose and P. K. Mascharak, *Coord. Chem. Rev.*, **2008**, 252, 2093–2114.
- 40 H.-J. Xiang, M. Guo, J.-G. Liu, *Eur. J. Inorg. Chem.*, **2017**, 1586-1597.
- 41 M. A. Evans, P.-J. Huang, Y. Iwamoto, K. N. Ibsen, E. M. Chan, Y. Hitomi, P. C. Ford, S. Mitragotri, *Chem. Sci.*, **2018**, 9, 3729-3741.
- 42 E. Tfouni, D. R. Truzzi, A. Tavare, A. J. Gomes, L. E. Figueiredo, D. W. Franco, *Nitric Oxide*, **2021**, 26, 38-53.
- 43 I. Stepanenko, M. Zalibera, D. Schaniel, J. Tesler, V. B. Arion, *Dalton Trans.*, **2022**, 51, 5367-5393.
- 44 J. H. Enemark and R. D. Feltham, *Coord. Chem. Rev.* 1974, **13**, 339-409.
- 45 A. F. Vanin, A. P. Poltorakov, V. D. Mikoyan, L. N. Kubrina, E. van Faassen, *Nitric Oxide* **2006**, 15, 295-311.
- 46 M. R. Hamblin, T. N. Demidova, *Proc. SPIE, Mech. Low-Light Therapy*, **2006**, 6140, 614001-614012.
- 47 T. R. de Boer, P. K. Mascharak, Pradip K., *Adv. Inorg. Chem.*, **2015**, 67, 145-170.
- 48 N. L. Fry, J. Wei, P. K. Mascharak, *Inorg. Chem.*, **2011**, 50, 9045-9052.
- 49 N. L. Fry, B. J. Heilman, P. K. Mascharak, Pradip K., *Inorg. Chem.*, **2011**, 50, 317-324.
- 50 F. Terenziani, C. Katan, E. Badaeva, S. Tretiak, M. Blanchard-Desce, *Adv. Mater.*, **2008**, 20, 4641-4678.
- 51 G. S. He, L.-S. Tan, Q. Zheng, P. N. Prasad, *Chem. Rev.*, **2008**, 108, 1245-1330.
- 52 Ch. Andraud, R. Fortrie, C. Barsu, O. Stéphan, H. Chermette, P. L. Baldeck, *Adv. Polym. Sci.*, **2008**, 214, 149-203.
- 53 B. J. Orr, J. F. Ward, *Mol. Phys.*, **1971**, 20, 513-526.
- 54 S. R. Weckler, A. Mikhailovsky, D. Korystov, P. C. Ford, *J. Am. Chem. Soc.*, **2006**, 128, 3831-3837.
- 55 S. R. Weckler, A. Mikhailovsky, D. Korystov, F. Buller, R. Kannan, L.-S. Tan, P. C. Ford, *Inorg. Chem.* **2007**, 46, 395-402.
- 56 Q. Zheng, A. Bonoiu, T. Ohulchanskyy, G. S. He, P. N. Prasad, *Mol. Pharma.*, **2008**, 5, 389-398.
- 57 S. Abid, Ch. Nguyen, M. Daurat, D. Durand, B. Jamoussi, M. Blanchard-Desce, M. Gary-Bobo, O. Mongin, Ch. O. Paul-Roth, F. Paul, *Dyes and Pigments* **2022**, 197, 109840.
- 58 C. Benitez-Martin, S. Li, A. Dominguez-Alfaro, F. Najera, E. Perez-Inestrosa, U. Pischel, J. Andreasson, *J. Am. Chem. Soc.* **2020**, 142, 14854-14858.
- 59 S. Goswami, S. Cekli, E. Alarousu, R. W. Winkel, M. Younus, O. F. Mohammed, K. S. Schanze, *Macromolecules* **2020**, 53, 6279-6287.
- 60 J.-W. Choi, S.-H. Choi, S. T. Hong, M. S. Kim, S. S. Ryu, Y. U. Yoon, K. C. Paik, M. S. Han, T. Sim, B. R. Cho, *Chem. Commun.* **2020**, 56, 3657-3660.

- 61 K. K. Guzman-Rabadan, M. Guizado-Rodriguez, V. Barba, M. Rodriguez, J. Velusamy, G. Ramos-Ortiz, *Opt. Mater.* **2020**, *101*, 109758.
- 62 J. Akl, I Sasaki, P.G. Lacroix, I. Malfant, S. Mallet-Ladeira, P. Vicendo, N. Farfán, R. Santillan, *Dalton Trans.*, **2014**, *45*, 12721-12733.
- 63 S. Amabilino, M. Tasse, P.G. Lacroix, S. Mallet-Ladeira, V. Pimienta, J. Akl, I. Sasaki, I. Malfant, *New J. Chem.*, **2017**, *41*, 7371-7383.
- 64 L. Khadeeva, W. Kaszub, M. Lorenc, I. Malfant, M. Buron-Le Cointe, *Inorg. Chem.* **2016**, *55*, 4117-4123.
- 65 L. Khadeeva, W. Kaszub, M. Lorenc, I. Malfant, M. Buron-Le Cointe, *Inorg. Chem.*, **2016**, *55*, 4117-4123.
- 66 A. Enriquez-Cabrera, I. Sasaki, V. Bukhanko, M. Tassé, S. Mallet-Ladeira, P.G. Lacroix, R.M. Barba-Barba, G. Ramos, N. Farfán, Z. Voitenko, I. Malfant, *Eur. J. Inorg. Chem.*, **2017**, 1446-1456.
- 67 J. Akl, I. Sasaki, P.G. Lacroix, V. Hugues, P. Vivendo, M. Bocé, S. Mallet-Ladeira, M. Blanchard-Desce, I. Malfant, *Photochem. Photobio. Sci.*, **2016**, *15*, 1484-1491.
- 68 D. Tsikas, *J. Chromatogr. B*, 2007, **851**, 51-70.
- 69 L. Wu, J. Liu, P. Li, B. Tang Bo, T.D. James Tony, *Chem. Soc. Rev.*, **2021**, *50*, 702-734.
- 70 C. Xu, W. W. Webb, *J. Opt. Soc. Am. B*, **1996**, *13*, 481-491.
- 71 E.W. Van Stryland, M. Sheik-Bahae, in *Characterization Techniques and Tabulations for Organic Nonlinear Materials* (Eds.: M.G. Kuzyk, C.W. Dirk), marcel Dekker, Inc., 1998, p.655-682.
- 72 M. Roose, I. Sasaki, V. Bukhanko, S. Mallet-Ladeira, R.M. Barba-Barba, G. Ramos-Ortiz, A. Enriquez-Cabrera, N. Farfán, P.G. Lacroix, I. Malfant, *Polyhedron*, **2018**, *151*, 100-111.
- 73 A. Enriquez-Cabrera, P.G. Lacroix, I. Sasaki, S. Malet-Ladeira, N. Farfan, R.M. Barba-Barba, G. Ramos-Ortiz, I. Malfant, *Eur. J. Inorg. Chem.*, **2018**, 531-543.
- 74 A. D. Laurent, D. Jacquemin, *Int. J. Quantum Chem.*, **2013**, *113*, 2019-2039.
- 75 B. Strehmel, A. M. Sarker, H. Detert, *ChemPhysChem*, **2003**, *4*, 249-259.
- 76 V. Bukhanko, A. F. León-Rojas, P. G. Lacroix, M. Tassé, G. Ramos-Ortiz, R. M. Barba-Barba, N. Farfán, R. Santillan, I. Malfant, *Eur. J. Inorg. Chem.*, **2021**, 1670-1684.
- 77 J. Zyss, I. Ledoux, *Chem. Rev.*, **1994**, *94*, 77-105.
- 78 Y. Juarez-Martinez, P. Labra-Vázquez, A. Enríquez-Cabrera, A.F. Leon-Rojas, D. Martínez-Bourget, P.G. Lacroix, M. Tassé, S. Mallet-Ladeira, N. Farfán, R. Santillan, G. Ramos-Ortiz, J.-P. Malval, I. Malfant, *Chem. Eur. J.*, **2022**, e202201692.
- 79 M. Romero-Ávila, A.F. León Rojas, P.G. Lacroix, I. Malfant, N. Farfan, R. Mhanna, R. Santillan, G. Ramos-Ortiz, J.-P. Malval, *J. Phys. Chem. Lett.*, **2020**, *11*, 6487-6491.

- 80 D. Beljonne, W. Wenseleers, E. Zojer, Z. Shuai, H. Vogel, S. J. K. Pond, J. W. Perry, S. R. Marder, J.-L. Brédas, *Adv. Funct. Mater.*, **2002**, *12*, 631-641.
- 81 L. Zhang, M. Morshedi, M. G. Humphrey, *Angew. Chem. Int. Ed.*, **2022**, *61*, e202116181 (1-5).
- 82 M. Bocé, M. Tassé, S. Mallet-Ladeira, F. Pillet, Ch. Da Silva, P. Vicendo, P.G. Lacroix, I. Malfant, M.P. Rols, *Scientific Reports*, **2019**, *9*, 4867, 1-8.